

Electroweak Corrections to the Decays of Stop and Gluino *

Hou Hong-Sheng^b, Ma Wen-Gan^{a,b}, Wan Lang-Hui^b and Zhang Ren-You^b

^a CCAST (World Laboratory), P.O.Box 8730, Beijing 100080,P.R.China

^b Department of Modern Physics, University of Science and Technology
of China (USTC), Hefei, Anhui 230027, P.R.China

Abstract

The electroweak corrections at the order of $O(\alpha_{ew} m_{t(b)}^2/m_W^2)$ to the partial widths of the $\tilde{t}_2 \rightarrow \tilde{g} + t$ and $\tilde{g} \rightarrow \tilde{t}_1 + \bar{t}$ decays (depending on the masses of the particles involved) are investigated within the Supersymmetric Standard Model. The relative corrections can reach the value of 10% in some parameter space, which can be comparable with the corresponding QCD corrections. Therefore, they should be taken into account for the precise experimental measurement at future colliders.

PACS: 11.30.Pb, 12.15.Lk, 12.60.Jv, 14.80.Ly

*Supported by National Natural Science Foundation of China.

1. INTRODUCTION

Over the past few years, many efforts have been devoted to search new physics beyond the standard model (SM) [1][2]. The minimal supersymmetric model(MSSM) [3] is considered as one of the most attractive extensions of the SM. Generally in the MSSM, two coloured scalar quarks (squarks) \tilde{q}_L and \tilde{q}_R , which correspond chiral eigenstates, are required as partners corresponding to the chiral quarks appearing in SM, because any realistic model must be extended from SM. The physical mass eigenstates \tilde{q}_1 and \tilde{q}_2 are the mixtures of these chiral eigenstates. Since in general the mixing size is proportional to the mass of the related ordinary quark [4], the mass splitting of the physical stop quarks \tilde{t}_1 and \tilde{t}_2 can be quite large. In fact, it is likely that the lighter stop mass eigenstate is the lightest scalar quark in supersymmetric theory and the mass $m_{\tilde{t}_1}$ may even be smaller than the top mass m_t itself [5]. This implies that there are quite different decay scenarios in the stop-top sector depending on the mass values of the particles involved. Therefore, the study of the scalar top quarks is of particular interest.

If the gluinos are heavy enough, scalar quarks will mainly decay into quarks plus chargino (or neutralino) and lighter squarks plus vector bosons (or Higgs bosons). These decays have been extensively discussed in the Born approximation [6][7]. The QCD corrections of the reaction $\tilde{q} \rightarrow q + \chi$ has been discussed in Ref.[8], and its inverse process: $t \rightarrow \tilde{t} + \chi^0$ and $t \rightarrow \tilde{b} + \chi^+$ have been discussed in Refs.[9]. The Yukawa corrections and the full one-loop electroweak(EW) radiative corrections to the squark decays into quarks plus charginos (or neutralinos) also were give in Refs.[10][11]. The QCD corrections and the Yukawa corrections to the heavier squark decays into lighter squarks plus vector bosons (or Higgs bosons) have been calculated in Refs.[12][13].

If stop particles are heavy enough ($m_{\tilde{t}_j} > m_t + m_{\tilde{g}}$), the decay pattern $\tilde{t}_j \rightarrow t + \tilde{g}$ will be kinematically allowed. The theoretical predictions of the SUSY-QCD corrections for the decay channels: $\tilde{q} \rightarrow \tilde{g} + q$ (for $m_{\tilde{q}} > m_{\tilde{g}} + m_q$), $\tilde{g} \rightarrow \tilde{q} + \bar{q}/\bar{\tilde{q}} + q$ (for $m_{\tilde{g}} > m_{\tilde{q}} + m_q$) have been calculated in Ref.[14], where q denotes quarks except top quark. And in Ref.[15], the processes: $\tilde{t}_j \rightarrow \tilde{g} + t$ and $\tilde{g} \rightarrow \tilde{t}_j + t$ are discussed including SUSY-QCD corrections.

Squarks and gluinos not heavier than a few hundred GeV , can be produced in significant number at high-energy hadron colliders, i.e. the Fermilab Tevatron $p\bar{p}$ collider and the LHC pp collider in the future [16][17]. In Ref.[18] it was argued that half of the top quark at Tevatron might come from gluino decays into top and stop, $\tilde{g} \rightarrow t + \tilde{t}_1$. So the accurate calculations including quantum corrections for these decays are necessary. The largest radiative corrections for the squark-gluino sector in the MSSM are associated with the strong interaction, the relative SUSY-QCD corrections for the process $\tilde{t}_2 \rightarrow \tilde{g} + t$ can reach 35% and that for $\tilde{g} \rightarrow \tilde{t}_1 + t$ can reach -10% [15]. However, the investigation of the electroweak corrections for these processes is necessary in precise experimental measurement, since their electroweak corrections maybe also sizable and could not be neglected. In this paper, we present the calculations of the Yukawa corrections of the order $O(\alpha_{ew} m_{t(b)}^2 / m_W^2)$ to the width of

$$\tilde{t}_2 \rightarrow \tilde{g} + t \quad (m_{\tilde{t}_2} > m_t + m_{\tilde{g}}) \quad (1)$$

$$\tilde{g} \rightarrow \bar{t} + \tilde{t}_1 \quad \text{and} \quad \text{c.c.} \quad (m_{\tilde{g}} > m_t + m_{\tilde{t}_1}) \quad (2)$$

These corrections are mainly induced by Yukawa couplings from Higgs-quark-quark couplings, Higgs-squark-squark couplings, Higgs-Higgs-squark-squark couplings, chargino (neutralino)-quark-squark couplings, and squark-squark-squark-squark couplings.

2. Notations and tree-level result

We summarize our notations and present the relevant interaction lagrangian of the MSSM as below in order to make our paper self-contained.

The tree-level stop squared-mass matrix is written as:

$$\begin{aligned} \mathcal{M}^2 &= \begin{pmatrix} \mathcal{M}_{LL}^2 & \mathcal{M}_{LR}^2 \\ \mathcal{M}_{RL}^2 & \mathcal{M}_{RR}^2 \end{pmatrix} \\ &= \begin{pmatrix} M_{\tilde{Q}}^2 + m_t^2 + m_Z^2 \cos 2\beta (\frac{1}{2} - \frac{2}{3} s_W^2) & -m_t (A_t + \mu \cot \beta) \\ -m_t (A_t + \mu \cot \beta) & M_{\tilde{U}}^2 + m_t^2 + \frac{2}{3} m_Z^2 \cos 2\beta s_W^2 \end{pmatrix} \end{aligned} \quad (3)$$

The parameters $M_{\tilde{Q}}$, $M_{\tilde{U}}$, μ and A_t are the soft-SUSY-breaking masses, SUSY Higgs mass parameter and trilinear coupling, m_Z and s_W are the Z-boson mass and the weak mixing angle, and $\tan\beta$ is the

ratio of the two vacuum expectation values in the Higgs sector. The diagonal entries of the stop mass matrix correspond to the L and R squark-mass terms, the off-diagonal entries are due to chirality-flip Yukawa interactions. The chiral states \tilde{t}_L and \tilde{t}_R are rotated into the mass eigenstates \tilde{t}_{10} and \tilde{t}_{20} :

$$\begin{pmatrix} \tilde{t}_{10} \\ \tilde{t}_{20} \end{pmatrix} = R^{\tilde{t}} \begin{pmatrix} \tilde{t}_L \\ \tilde{t}_R \end{pmatrix}, \quad R^{\tilde{t}} = \begin{pmatrix} \cos \theta_0 & \sin \theta_0 \\ -\sin \theta_0 & \cos \theta_0 \end{pmatrix} \quad (4)$$

by these Yukawa interactions. The mass eigenvalues and the rotation angle can be calculated from the mass matrix in Eq.(3):

$$m_{\tilde{t}_1}^2, m_{\tilde{t}_2}^2 = \frac{1}{2} \left[\mathcal{M}_{LL}^2 + \mathcal{M}_{RR}^2 \mp \left[(\mathcal{M}_{LL}^2 - \mathcal{M}_{RR}^2)^2 + 4(\mathcal{M}_{LR}^2)^2 \right]^{1/2} \right] \quad (5)$$

$$\sin(2\theta_0) = \frac{2\mathcal{M}_{LR}^2}{m_{\tilde{t}_1}^2 - m_{\tilde{t}_2}^2}, \quad \cos(2\theta_0) = \frac{(\mathcal{M}_{LL}^2 - \mathcal{M}_{RR}^2)}{m_{\tilde{t}_1}^2 - m_{\tilde{t}_2}^2}, \quad (6)$$

where we assume \tilde{t}_1 to be the lighter stop state.

We can write the relevant lagrangian density in the $(\tilde{t}_L, \tilde{t}_R)$ basis as following form (a, j, k are colour indices):

$$\mathcal{L} = -\sqrt{2}\hat{g}_s T_{jk}^a \left(\bar{\tilde{g}}_a P_L t^k \tilde{t}_L^{j*} + \bar{t}^j P_R \tilde{g}_a \tilde{t}_L^k - \bar{\tilde{g}}_a P_R t^k \tilde{t}_R^{j*} - \bar{t}^j P_L \tilde{g}_a \tilde{t}_R^k \right) \quad (7)$$

Here the $q\tilde{q}\tilde{g}$ Yukawa coupling \hat{g}_s should coincide with the qqg gauge coupling g_s by supersymmetry.

The tree-level partial widths for the stop and gluino decays, $\tilde{t}_{1,2} \rightarrow \tilde{g} + t$ and $\tilde{g} \rightarrow \tilde{t}_{1,2} + t$ as shown in Fig.1(a.1)-(a.3), are given by [15]:

$$\Gamma_0(\tilde{t}_{1,2} \rightarrow \tilde{g}t) = \frac{2\alpha_s \kappa}{3m_{\tilde{t}_{1,2}}^3} \left[m_{\tilde{t}_{1,2}}^2 - m_t^2 - m_{\tilde{g}}^2 \pm 2m_t m_{\tilde{g}} \sin(2\theta_0) \right] \quad (8)$$

$$\Gamma_0(\tilde{g} \rightarrow \tilde{t}\tilde{t}_{1,2}) = -\frac{\alpha_s \kappa}{8m_{\tilde{g}}^3} \left[m_{\tilde{t}_{1,2}}^2 - m_t^2 - m_{\tilde{g}}^2 \pm 2m_t m_{\tilde{g}} \sin(2\theta_0) \right] \quad (9)$$

where

$$\kappa = \left(\sum_i m_i^4 - \sum_{i \neq j} m_i^2 m_j^2 \right)^{1/2} \quad (10)$$

The sums run over all particles involved in the decay process.

3. Yukawa corrections

The Feynman diagrams of the one-loop Yukawa corrections to the processes (1) and (2) are shown in Figs.1(b.1)-(b.4). In the calculation, we use the t'Hooft gauge and adopt the dimensional reduction scheme(DR)[19], which is commonly used in the calculation of the electroweak correction in frame of the MSSM as it preserves supersymmetry at least at one-loop order, to control the ultraviolet divergences in the virtual loop corrections. The complete on-mass-shell scheme [20][21] is used in doing renormalization.

The relevant renormalization constants are defined as

$$\begin{aligned} t_0 &= \left(1 + \frac{1}{2}\delta Z_{tt}^L P_L + \frac{1}{2}\delta Z_{tt}^R P_R\right) t \\ \tilde{t}_{i0} &= \left(1 + \delta Z_i^{\tilde{t}}\right)^{1/2} \tilde{t}_i + \delta Z_{ij}^{\tilde{t}} \tilde{t}_j \\ \theta_0 &= \theta + \delta\theta \end{aligned} \quad (11)$$

In the on-mass-shell scheme the renormalization constants defined in Eq.(11) can be fixed by the renormalization conditions[20][21] as:

$$\begin{aligned} \delta Z_{tt}^L &= -\tilde{R}e \left[\Sigma_{tt}^L(m_t^2) + m_t^2(\Sigma_{tt}^{L'}(m_t^2) + \Sigma_{tt}^{R'}(m_t^2)) + m_t(\Sigma_{tt}^{SL'}(m_t^2) + \Sigma_{tt}^{SR'}(m_t^2)) \right], \\ \delta Z_{tt}^R &= -\tilde{R}e \left[\Sigma_{tt}^R(m_t^2) + m_t^2(\Sigma_{tt}^{L'}(m_t^2) + \Sigma_{tt}^{R'}(m_t^2)) + m_t(\Sigma_{tt}^{SL'}(m_t^2) + \Sigma_{tt}^{SR'}(m_t^2)) \right] \end{aligned} \quad (12)$$

where $\Sigma'(m_t^2) = \frac{\partial \Sigma(p^2)}{\partial p^2}|_{p^2=m_t^2}$. Notice that the stop wave-function renormalization involves the mixed scalar field renormalization constants:

$$\begin{aligned} \delta Z_i^{\tilde{t}} &= -\tilde{R}e \Sigma_{ii}^{\tilde{t}}(m_{\tilde{t}_i}^2), \\ \delta Z_{ij}^{\tilde{t}} &= \frac{\Sigma_{ij}^{\tilde{t}}(m_{\tilde{t}_j}^2)}{m_{\tilde{t}_j}^2 - m_{\tilde{t}_i}^2} \quad (i \neq j) \end{aligned} \quad (13)$$

For the counterterm of stop mixing angle θ , using the same renormalization scheme as Ref.[10], we can get:

$$\delta\theta = \frac{1}{2}(\delta Z_{12}^{\tilde{t}} - \delta Z_{21}^{\tilde{t}}) = \frac{1}{2} \frac{\Sigma_{12}^{\tilde{t}}(m_{\tilde{t}_1}^2) + \Sigma_{12}^{\tilde{t}}(m_{\tilde{t}_2}^2)}{m_{\tilde{t}_2}^2 - m_{\tilde{t}_1}^2} \quad (14)$$

Taking into account the Yukawa corrections, the renormalized amplitude for these process is given by

$$M_{ren} = M_0 + \delta M \quad (15)$$

Correspondingly, the renormalized decay width is then given by

$$\Gamma_{ren} = \Gamma_0 + \delta\Gamma \quad (16)$$

In the following we present the explicit calculation of the decay width of $\tilde{t}_2 \rightarrow t\tilde{g}$, while the calculation for the decays of $\tilde{t}_1 \rightarrow t\tilde{g}$ and $\tilde{g} \rightarrow \tilde{t}\tilde{t}$ are very similar with that for $\tilde{t}_2 \rightarrow t\tilde{g}$, so we will not present them. Now we present the explicit formulae of the calculation of the process $\tilde{t}_2 \rightarrow t\tilde{g}$.

We denote this process as:

$$\tilde{t}_2(p_1, c_1) \rightarrow t(k_1, c_2) + \tilde{g}(k_2, a) \quad (17)$$

where c_1, c_2, a are colour indices. By substituting Eq.(11) into the bare Lagrangian, we can obtain its counterterm.

$$\begin{aligned} \delta\mathcal{L}_{\tilde{t}_2 t\tilde{g}} &\equiv -\sqrt{2}\hat{g}_s T_{c_1 c_2}^a \bar{t} [\delta C_L P_L + \delta C_R P_R] \tilde{g} \tilde{t}_2 \\ &= -\sqrt{2}\hat{g}_s T_{c_1 c_2}^a \bar{t} \left[\left(-\delta Z_{12}^{\tilde{t}} \sin\theta - \frac{1}{2}\delta Z_{tt}^{R*} \cos\theta - \frac{1}{2}\delta Z_2^{\tilde{t}} \cos\theta + \delta\theta \sin\theta \right) R_L \right. \\ &\quad \left. + \left(\delta Z_{12}^{\tilde{t}} \cos\theta - \frac{1}{2}\delta Z_{tt}^{L*} \sin\theta - \frac{1}{2}\delta Z_2^{\tilde{t}} \sin\theta - \delta\theta \cos\theta \right) P_R \right] \end{aligned} \quad (18)$$

Then the renormalized one-loop part of the amplitude for the decay $\tilde{t}_2 \rightarrow t + \tilde{g}$ can be written as

$$\delta\mathcal{M} = \delta\mathcal{M}^c + \delta\mathcal{M}^v, \quad (19)$$

where $\delta\mathcal{M}^v$ and $\delta\mathcal{M}^c$ are contributed by the vertex corrections and the counterterm, respectively. They have the expressions as:

$$\begin{aligned} \delta\mathcal{M}^c &= -i\sqrt{2}\hat{g}_s T_{c_1 c_2}^a \bar{t} [\delta C_L P_L + \delta C_R P_R] \tilde{g} \tilde{t}_2 \\ \delta\mathcal{M}^v &= T_{c_1 c_2}^a \bar{t} [\Lambda_1 + \Lambda_2 \gamma_5] \tilde{g} \tilde{t}_2 \end{aligned} \quad (20)$$

$\delta C_{L,R}$ are defined in Eq.(18), and $\Lambda_{1,2}$ are the form factors contributed by the diagrams in Fig.1(b).

We decompose the form factors $\Lambda_{1,2}$ in the form as:

$$\Lambda_{1,2} = \Lambda_{1,2}^{(1)} + \Lambda_{1,2}^{(2)} + \Lambda_{1,2}^{(3)} + \Lambda_{1,2}^{(4)}, \quad (21)$$

where $\Lambda_{1,2}^{(i)}$ ($i = 1, 2, 3, 4$) are the form factors contributed by the diagrams in Fig.1(b.1), Fig.1(b.2), Fig.1(b.3) and Fig.1(b.4), respectively.

- For diagram Fig.1(b.1), we introduce the following notations:

$$\begin{aligned} F_a^{(1)} &= V_{\tilde{g}b_\beta b}^{(1)*} V_{t\tilde{b}_\beta \tilde{\chi}_k^+}^{(1)} V_{b\tilde{t}_2 \tilde{\chi}_k^+}^{(1)}, & F_b^{(1)} &= V_{\tilde{g}b_\beta b}^{(2)*} V_{t\tilde{b}_\beta \tilde{\chi}_k^+}^{(1)} V_{b\tilde{t}_2 \tilde{\chi}_k^+}^{(1)}, \\ F_c^{(1)} &= V_{\tilde{g}b_\beta b}^{(1)*} V_{t\tilde{b}_\beta \tilde{\chi}_k^+}^{(2)} V_{b\tilde{t}_2 \tilde{\chi}_k^+}^{(1)}, & F_d^{(1)} &= V_{\tilde{g}b_\beta b}^{(2)*} V_{t\tilde{b}_\beta \tilde{\chi}_k^+}^{(2)} V_{b\tilde{t}_2 \tilde{\chi}_k^+}^{(1)}, \\ F_e^{(1)} &= V_{\tilde{g}b_\beta b}^{(1)*} V_{t\tilde{b}_\beta \tilde{\chi}_k^+}^{(1)} V_{b\tilde{t}_2 \tilde{\chi}_k^+}^{(2)}, & F_f^{(1)} &= V_{\tilde{g}b_\beta b}^{(2)*} V_{t\tilde{b}_\beta \tilde{\chi}_k^+}^{(1)} V_{b\tilde{t}_2 \tilde{\chi}_k^+}^{(2)}, \\ F_g^{(1)} &= V_{\tilde{g}b_\beta b}^{(1)*} V_{t\tilde{b}_\beta \tilde{\chi}_k^+}^{(2)} V_{b\tilde{t}_2 \tilde{\chi}_k^+}^{(2)}, & F_h^{(1)} &= V_{\tilde{g}b_\beta b}^{(2)*} V_{t\tilde{b}_\beta \tilde{\chi}_k^+}^{(2)} V_{b\tilde{t}_2 \tilde{\chi}_k^+}^{(2)}. \end{aligned} \quad (22)$$

The form factors $\Lambda_{1,2}^{(1)}$ contributed by diagram Fig.1(b.1) are:

$$\begin{aligned} \Lambda_1^{(1)} &= \frac{1}{32\pi^2} \sum_{k,\beta=1}^2 \left[\left(m_t m_{\tilde{\chi}_k^+} (F_a^{(1)} + F_h^{(1)}) + (m_t^2 + m_t m_{\tilde{g}}) (F_c^{(1)} + F_f^{(1)}) + m_t m_b (F_d^{(1)} + F_e^{(1)}) \right) C_{11}^{(1)} \right. \\ &+ \left. \left((m_{\tilde{g}} - m_t) m_{\tilde{\chi}_k^+} (F_a^{(1)} + F_h^{(1)}) + (m_{\tilde{g}}^2 - m_t^2) (F_c^{(1)} + F_f^{(1)}) + (m_{\tilde{g}} - m_t) m_b (F_d^{(1)} + F_e^{(1)}) \right) C_{12}^{(1)} \right. \\ &+ \left. \left(m_{\tilde{g}} m_{\tilde{\chi}_k^+} (F_a^{(1)} + F_h^{(1)}) + m_{\tilde{\chi}_k^+} m_b (F_b^{(1)} + F_g^{(1)}) + (m_t m_{\tilde{g}} + m_{\tilde{b}_\beta}^2) (F_c^{(1)} + F_f^{(1)}) \right. \right. \\ &+ \left. \left. m_t m_b (F_d^{(1)} + F_e^{(1)}) \right) C_0^{(1)} - \left(F_c^{(1)} + F_f^{(1)} \right) B_0^{(1)} \right] \\ \Lambda_2^{(1)} &= \frac{1}{32\pi^2} \sum_{k,\beta=1}^2 \left[\left(m_t m_{\tilde{\chi}_k^+} (F_a^{(1)} - F_h^{(1)}) + (m_t^2 - m_t m_{\tilde{g}}) (F_c^{(1)} - F_f^{(1)}) + m_t m_b (F_e^{(1)} - F_d^{(1)}) \right) C_{11}^{(1)} \right. \\ &+ \left. \left((m_t + m_{\tilde{g}}) m_{\tilde{\chi}_k^+} (F_h^{(1)} - F_a^{(1)}) + (m_t^2 - m_{\tilde{g}}^2) (F_f^{(1)} - F_c^{(1)}) + (m_t + m_{\tilde{g}}) m_b (F_d^{(1)} - F_e^{(1)}) \right) C_{12}^{(1)} \right. \\ &+ \left. \left(m_{\tilde{g}} m_{\tilde{\chi}_k^+} (F_h^{(1)} - F_a^{(1)}) + m_{\tilde{\chi}_k^+} m_b (F_g^{(1)} - F_b^{(1)}) + (m_t m_{\tilde{g}} - m_{\tilde{b}_\beta}^2) (F_f^{(1)} - F_c^{(1)}) \right. \right. \\ &+ \left. \left. m_t m_b (F_e^{(1)} - F_d^{(1)}) \right) C_0^{(1)} + \left(F_f^{(1)} - F_c^{(1)} \right) B_0^{(1)} \right] \end{aligned} \quad (23)$$

with $B_0^{(1)} = B_0(-p_1, m_{\tilde{\chi}_k^+}, m_b)$, $C_{0,11,12}^{(1)} = C_{0,11,12}(k_1, -p_1, m_{\tilde{b}_\beta}, m_{\tilde{\chi}_k^+}, m_b)$.

- For diagram Fig.1(b.2), we introduce the following notations:

$$\begin{aligned}
F_a^{(2)} &= V_{\tilde{g}\tilde{t}_\alpha t}^{(1)*} V_{tt_2\tilde{\chi}_l^0}^{(1)} V_{t\tilde{t}_\alpha\tilde{\chi}_l^0}^{(1)}, & F_b^{(2)} &= V_{\tilde{g}\tilde{t}_\alpha t}^{(2)*} V_{tt_2\tilde{\chi}_l^0}^{(1)} V_{t\tilde{t}_\alpha\tilde{\chi}_l^0}^{(1)}, \\
F_c^{(2)} &= V_{\tilde{g}\tilde{t}_\alpha t}^{(1)*} V_{tt_2\tilde{\chi}_l^0}^{(2)} V_{t\tilde{t}_\alpha\tilde{\chi}_l^0}^{(1)}, & F_d^{(2)} &= V_{\tilde{g}\tilde{t}_\alpha t}^{(2)*} V_{tt_2\tilde{\chi}_l^0}^{(2)} V_{t\tilde{t}_\alpha\tilde{\chi}_l^0}^{(1)}, \\
F_e^{(2)} &= V_{\tilde{g}\tilde{t}_\alpha t}^{(1)*} V_{tt_2\tilde{\chi}_l^0}^{(1)} V_{t\tilde{t}_\alpha\tilde{\chi}_l^0}^{(2)}, & F_f^{(2)} &= V_{\tilde{g}\tilde{t}_\alpha t}^{(2)*} V_{tt_2\tilde{\chi}_l^0}^{(1)} V_{t\tilde{t}_\alpha\tilde{\chi}_l^0}^{(2)}, \\
F_g^{(2)} &= V_{\tilde{g}\tilde{t}_\alpha t}^{(1)*} V_{tt_2\tilde{\chi}_l^0}^{(2)} V_{t\tilde{t}_\alpha\tilde{\chi}_l^0}^{(2)}, & F_h^{(1)} &= V_{\tilde{g}\tilde{t}_\alpha t}^{(2)*} V_{tt_2\tilde{\chi}_l^0}^{(2)} V_{t\tilde{t}_\alpha\tilde{\chi}_l^0}^{(2)}. \tag{24}
\end{aligned}$$

The form factors $\Lambda_{1,2}^{(2)}$ contributed by diagram Fig.1(b.2) are:

$$\begin{aligned}
\Lambda_1^{(2)} &= \frac{1}{32\pi^2} \sum_{l=1}^4 \sum_{\alpha=1}^2 \left[\left(m_t m_{\tilde{\chi}_l^0} (F_a^{(2)} + F_h^{(2)}) + m_t^2 (F_c^{(2)} + F_f^{(2)}) + (m_t^2 + m_t m_{\tilde{g}}) (F_d^{(2)} + F_e^{(2)}) \right) C_{11}^{(2)} \right. \\
&+ \left. \left((m_{\tilde{g}} - m_t) m_{\tilde{\chi}_l^0} (F_a^{(2)} + F_h^{(2)}) + (m_{\tilde{g}} - m_t) m_t (F_c^{(2)} + F_f^{(2)}) + (m_{\tilde{g}}^2 - m_t^2) (F_d^{(2)} + F_e^{(2)}) \right) C_{12}^{(2)} \right. \\
&+ \left. \left(m_{\tilde{g}} m_{\tilde{\chi}_l^0} (F_a^{(2)} + F_h^{(2)}) + m_{\tilde{\chi}_l^0} m_t (F_b^{(2)} + F_g^{(2)}) + m_t^2 (F_c^{(2)} + F_f^{(2)}) \right. \right. \\
&+ \left. \left. (m_t m_{\tilde{g}} + m_{\tilde{t}_\alpha}^2) (F_d^{(2)} + F_e^{(2)}) \right) C_0^{(2)} - (F_d^{(2)} + F_e^{(2)}) B_0^{(2)} \right] \\
\Lambda_2^{(2)} &= \frac{1}{32\pi^2} \sum_{l=1}^4 \sum_{\alpha=1}^2 \left[\left(m_t m_{\tilde{\chi}_l^0} (F_a^{(2)} - F_h^{(2)}) + m_t^2 (F_c^{(2)} - F_f^{(2)}) + (m_t m_{\tilde{g}} - m_t^2) (F_d^{(2)} - F_e^{(2)}) \right) C_{11}^{(2)} \right. \\
&+ \left. \left((m_t + m_{\tilde{g}}) m_{\tilde{\chi}_l^0} (F_h^{(2)} - F_a^{(2)}) + (m_t + m_{\tilde{g}}) m_t (F_f^{(2)} - F_c^{(2)}) + (m_t^2 - m_{\tilde{g}}^2) (F_d^{(2)} - F_e^{(2)}) \right) C_{12}^{(2)} \right. \\
&+ \left. \left(m_{\tilde{g}} m_{\tilde{\chi}_l^0} (F_h^{(2)} - F_a^{(2)}) + m_{\tilde{\chi}_l^0} m_t (F_g^{(2)} - F_b^{(2)}) + m_t^2 (F_c^{(2)} - F_f^{(2)}) \right. \right. \\
&+ \left. \left. (m_t m_{\tilde{g}} - m_{\tilde{t}_\alpha}^2) (F_d^{(2)} - F_e^{(2)}) \right) C_0^{(2)} + (F_d^{(2)} - F_e^{(2)}) B_0^{(2)} \right] \tag{25}
\end{aligned}$$

with $B_0^{(2)} = B_0(-p_1, m_{\tilde{\chi}_l^0}, m_t)$, $C_{0,11,12}^{(2)} = C_{0,11,12}(k_1, -p_1, m_{\tilde{t}_\alpha}, m_{\tilde{\chi}_l^0}, m_t)$.

- For diagram Fig.1(b.3), we introduce the following notations:

$$F_a^{(3)} = V_{H_m^0 tt} V_{H_m^0 \tilde{t}_\alpha \tilde{t}_2} V_{\tilde{g}\tilde{t}_\alpha t}^{(1)}, \quad F_b^{(3)} = V_{H_m^0 tt} V_{H_m^0 \tilde{t}_\alpha \tilde{t}_2} V_{\tilde{g}\tilde{t}_\alpha t}^{(2)} \tag{26}$$

The form factors $\Lambda_{1,2}^{(3)}$ contributed by diagram Fig.1(b.3) are:

$$\begin{aligned}
\Lambda_1^{(3)} &= \frac{1}{32\pi^2} \sum_m^4 \left[(F_a^{(3)} - F_b^{(3)}) (m_t (C_0^{(3)} + C_{11}^{(3)} - C_{12}^{(3)}) + m_{\tilde{g}} C_{12}^{(3)}) \right] \\
\Lambda_2^{(3)} &= \frac{1}{32\pi^2} \sum_m^4 \left[-(F_a^{(3)} + F_b^{(3)}) m_t (C_0^{(3)} + C_{11}^{(3)} - C_{12}^{(3)}) + m_{\tilde{g}} C_{12}^{(3)} \right] \tag{27}
\end{aligned}$$

with $C_{0,11,12}^{(3)} = C_{0,11,12}(k_1, -p_1, m_t, m_{H_m^0}, m_{\tilde{t}_\alpha})$

- For diagram Fig.1(b.4), we introduce the following notations:

$$\begin{aligned}
F_a^{(4)} &= V_{H_n^+ tb}^{(1)} V_{H_n^+ \tilde{t}_2 \tilde{b}_\beta}^* V_{\tilde{g} \tilde{b}_\beta b}^{(1)}, & F_b^{(4)} &= V_{H_n^+ tb}^{(2)} V_{H_n^+ \tilde{t}_2 \tilde{b}_\beta}^* V_{\tilde{g} \tilde{b}_\beta b}^{(1)} \\
F_c^{(4)} &= V_{H_n^+ tb}^{(1)} V_{H_n^+ \tilde{t}_2 \tilde{b}_\beta}^* V_{\tilde{g} \tilde{b}_\beta b}^{(2)}, & F_d^{(4)} &= V_{H_n^+ tb}^{(2)} V_{H_n^+ \tilde{t}_2 \tilde{b}_\beta}^* V_{\tilde{g} \tilde{b}_\beta b}^{(2)}
\end{aligned} \tag{28}$$

The form factors $\Lambda_{1,2}^{(4)}$ contributed by diagram Fig.1(b.4) are:

$$\begin{aligned}
\Lambda_1^{(4)} &= \frac{1}{32\pi^2} \sum_n^2 \left[m_b (F_a^{(4)} + F_d^{(4)}) C_0^{(4)} - m_t (F_b^{(4)} + F_c^{(4)}) C_{11}^{(4)} + (m_t - m_{\tilde{g}}) (F_b^{(4)} + F_c^{(4)}) C_{12}^{(4)} \right] \\
\Lambda_2^{(4)} &= \frac{1}{32\pi^2} \sum_n^2 \left[m_b (F_d^{(4)} - F_a^{(4)}) C_0^{(4)} - m_t (F_c^{(4)} - F_b^{(4)}) C_{11}^{(4)} + (m_t - m_{\tilde{g}}) (F_c^{(4)} - F_b^{(4)}) C_{12}^{(4)} \right]
\end{aligned} \tag{29}$$

with $C_{0,11,12}^{(4)} = C_{0,11,12}(k_1, -p_1, m_b, m_{H_n^+}, m_{\tilde{b}_\beta})$

4. Numerical results and conclusion

In the numerical analysis, we take the SM input parameters as: $m_t = 174.3 \text{ GeV}$, $m_b = 4.3 \text{ GeV}$, $m_Z = 91.1882 \text{ GeV}$, $m_W = 80.419 \text{ GeV}$ and $\alpha_{EW} = 1/128$ [22].

Fig.2 shows the dependence on $m_{\tilde{g}}$ of the relative correction $\delta\Gamma/\Gamma_0$ for the decay $\tilde{t}_2 \rightarrow t + \tilde{g}$. For simple, we assumed $M_{\tilde{Q}} = M_{\tilde{U}} = M_{\tilde{D}} = A_t = A_b = M_{susy}$. The ratio of the vacuum expectation values $\tan \beta$ is set to be 4. The mass of charged Higgs boson $m_{H^\pm} = 250 \text{ GeV}$. The physical chargino masses $m_{\tilde{\chi}_1^\pm}$, $m_{\tilde{\chi}_2^\pm}$ and the lightest neutralino mass $m_{\tilde{\chi}_1^0}$ are set to be 100 GeV, 300 GeV and 60 GeV, respectively. Then the fundamental SUSY parameters M , M' and μ in the chargino and neutralino matrix can be extracted from these input chargino masses, lightest neutralino mass $m_{\tilde{\chi}_1^0}$ and $\tan \beta$. The solid curve is for $M_{susy} = 400 \text{ GeV}$ and the dashed curve is for $M_{susy} = 500 \text{ GeV}$. We can see the relative Yukawa correction to this process is always negative when the $m_{\tilde{g}}$ is in the range 80 to 300 GeV. The figure shows that the relative Yukawa correction is not very sensitive to the value of $m_{\tilde{g}}$ and has the values about -3% .

In Fig.3 we present the numerical result of the Yukawa correction for the decay $\tilde{t}_2 \rightarrow t + \tilde{g}$ in the mSUGRA scenario. The squark masses and mixing parameters are calculated from the input

mSUGRA parameters: the common scalar mass m_0 , the common gaugino mass $m_{1/2}$, the trilinear coupling A_0 , the ratio of the vacuum expectation values of the Higgs fields $\tan\beta$, and the sign of the Higgsino mass parameter μ . Here we take $m_0 = 800 \text{ GeV}$, $A_0 = 200 \text{ GeV}$, and $\tan\beta = 1.75$. The solid curve is for $\mu > 0$ and the dashed curve is for $\mu < 0$. In the case of $\mu < 0$ and $m_{1/2} > 195 \text{ GeV}$, the decay $\tilde{t}_2 \rightarrow t + \tilde{g}$ cannot be opened kinematically in the mSUGRA model. While in the case of $\mu > 0$ and $m_{1/2} > 210 \text{ GeV}$, the decay $\tilde{t}_2 \rightarrow t + \tilde{g}$ is forbidden. The figure shows that the relative Yukawa correction to this process varies between -9% to -2% for $\mu > 0$ and between -6% to -3% for $\mu < 0$.

Fig.4 shows the dependence on $m_{\tilde{g}}$ of the relative correction for the decay $\tilde{g} \rightarrow \bar{t} + \tilde{t}_1$. Here we choose $\tan\beta = 4$, and $m_{H^\pm} = 250 \text{ GeV}$. The physical chargino masses $m_{\tilde{\chi}_1^\pm}$, $m_{\tilde{\chi}_2^\pm}$ and the lightest neutralino mass $m_{\tilde{\chi}_1^0}$ are set to be 100 GeV , 300 GeV and 60 GeV , respectively. In Fig.4 the solid curve is for $M_{susy} = 200 \text{ GeV}$ and the dashed curve is for $M_{susy} = 150 \text{ GeV}$. The relative Yukawa correction to this example decreases from 1% to -4% with the increasing of $m_{\tilde{g}}$ from 400 to 800 GeV .

In Fig.5 we present the numerical result of the Yukawa correction for the decay $\tilde{g} \rightarrow \bar{t} + \tilde{t}_1$ in the mSUGRA scenario. In this example we take $m_0 = 400 \text{ GeV}$, $A_0 = 200 \text{ GeV}$, and $\tan\beta = 1.75$. The solid curve and dashed curve are for $\mu > 0$ and $\mu < 0$, respectively. The figure shows that when $\mu < 0$ and $m_{1/2} < 237 \text{ GeV}$, the decay $\tilde{g} \rightarrow \bar{t} + \tilde{t}_1$ is not allowed kinematically, and when $\mu > 0$ and $m_{1/2} < 145 \text{ GeV}$, this decay is closed in the mSUGRA scenario. We can see that in the case of $\mu > 0$, the relative Yukawa correction is always negative and varies from -5% to -1% . For $\mu < 0$, the relative correction decreases from 10% to -2% with the increasing of $m_{1/2}$ from 145 GeV to 400 GeV .

In Summary, we have computed the one-loop electroweak Yukawa corrections to the partial widths of the $\tilde{t}_2 \rightarrow t + \tilde{g}$ and $\tilde{g} \rightarrow \bar{t} + \tilde{t}_1$ decays within the Minimal Supersymmetric Standard Model. We find that the relative corrections can be significant and reach the value of 10% in some parameter space, which can be comparable with the corresponding QCD corrections. Therefore, the electroweak corrections to these decays of scalar top quark and gluino should be taken into account in the precise experiment measurements.

Acknowledgement: This work was supported in part by the National Natural Science Foundation

of China and the Education Ministry of China.

Appendix A

In this Appendix, we list the self-energies of stop quark and top quark contributed by Fig.1(c) and Fig.1(d). The relevant Feynman rules are presented in Ref.[3] [4]. We adopt the notations of the couplings that chargino (neutralino) coupling with quark and squark in Ref.[23]. They are written as bellow:

$$\begin{aligned} \bar{b} - \tilde{t}_i - \tilde{\chi}_j^+ &: \left(V_{b\tilde{t}_i\tilde{\chi}_j^+}^{(1)} P_L + V_{b\tilde{t}_i\tilde{\chi}_j^+}^{(2)} P_R \right) C, \quad \bar{t} - \tilde{b}_i - \tilde{\chi}_j^+ : V_{t\tilde{b}_i\tilde{\chi}_j^+}^{(1)} P_L + V_{t\tilde{b}_i\tilde{\chi}_j^+}^{(2)} P_R, \\ \bar{b} - \tilde{b}_i - \tilde{\chi}_j^0 &: V_{b\tilde{b}_i\tilde{\chi}_j^0}^{(1)} P_L + V_{b\tilde{b}_i\tilde{\chi}_j^0}^{(2)} P_R, \quad \bar{t} - \tilde{t}_i - \tilde{\chi}_j^0 : V_{t\tilde{t}_i\tilde{\chi}_j^0}^{(1)} P_L + V_{t\tilde{t}_i\tilde{\chi}_j^0}^{(2)} P_R, \end{aligned} \quad (\text{A.1})$$

where C is the charge conjugation operator.

Defining $H_m^0 = (h^0, H^0, A^0, G^0)$ ($m = 1, 2, 3, 4$) and $H_n^\pm = (H^\pm, G^\pm)$ ($n = 1, 2$), the couplings between H_m^0 (H_n^\pm) and quark(squark) are denoted as:

$$\begin{aligned} H_n^+ - \bar{t} - b &: V_{H_n^+ tb}^{(1)} P_L + V_{H_n^+ tb}^{(2)} P_R, \quad H_n^+ - \tilde{t}_i - \tilde{b}_j : V_{H_n^+ \tilde{t}_i \tilde{b}_j}, \\ H_n^+ - H_n^- - \tilde{t}_i - \tilde{t}_j &: V_{H_n^+ H_n^- \tilde{t}_i \tilde{t}_j}, \\ H_m^0 - \bar{t} - t &: V_{H_m^0 tt} \quad (\text{for } m = 1, 2); \quad \gamma_5 V_{H_m^0 tt} \quad (\text{for } m = 3, 4), \\ H_m^0 - \tilde{t}_i - \tilde{t}_j &: V_{H_m^0 \tilde{t}_i \tilde{t}_j}, \quad H_m^0 - H_m^0 - \tilde{t}_i - \tilde{t}_j : V_{H_m^0 H_m^0 \tilde{t}_i \tilde{t}_j}. \end{aligned} \quad (\text{A.2})$$

The couplings between four squarks are denoted as:

$$\tilde{t}_i - \tilde{t}_j - \tilde{t}_k - \tilde{t}_l : V_{\tilde{t}_i \tilde{t}_j \tilde{t}_k \tilde{t}_l} \quad \tilde{t}_i - \tilde{t}_j - \tilde{b}_k - \tilde{b}_l : V_{\tilde{t}_i \tilde{t}_j \tilde{b}_k \tilde{b}_l} \quad (\text{A.3})$$

And we denote the couplings between gluino, quark and squark as:

$$\tilde{g} - \tilde{t}_i - \bar{t} : V_{\tilde{g}\tilde{t}_i t}^{(1)} P_L + V_{\tilde{g}\tilde{t}_i t}^{(2)} P_R \quad \tilde{g} - \tilde{b}_i - \bar{b} : V_{\tilde{g}\tilde{b}_i b}^{(1)} P_L + V_{\tilde{g}\tilde{b}_i b}^{(2)} P_R \quad (\text{A.4})$$

The stop quark self-energy contributed by Fig.1(c1)-(c3) reads:

$$\Sigma_{ij}^{\tilde{t}}(p^2) = \frac{1}{16\pi^2} \left\{ \sum_m^4 \sum_{\alpha}^2 \left[-2iA_0(m_{H_m^0}) V_{H_m^0 H_m^0 \tilde{t}_i \tilde{t}_j} - B_0(-p, m_{\tilde{t}_\alpha}, m_{H_m^0}) V_{H_m^0 \tilde{t}_j \tilde{t}_\alpha} V_{H_m^0 \tilde{t}_\alpha \tilde{t}_i} \right] \right\}$$

$$\begin{aligned}
& - \sum_n^2 \sum_\beta^2 \left[i A_0(m_{H_n^+}) V_{H_n^+ H_n^- \tilde{t}_i \tilde{t}_j} + B_0(-p, m_{\tilde{b}_\beta}, m_{H_n^+}) V_{H_n^+ \tilde{t}_i \tilde{b}_\beta} V_{H_n^+ \tilde{t}_j \tilde{b}_\beta} \right] \\
& - \sum_l^4 \left[2 \left(V_{t \tilde{t}_j \tilde{\chi}_l^0}^{(1)*} V_{t \tilde{t}_i \tilde{\chi}_l^0}^{(1)} + V_{t \tilde{t}_j \tilde{\chi}_l^0}^{(2)*} V_{t \tilde{t}_i \tilde{\chi}_l^0}^{(2)} \right) \left(A_0(m_{\tilde{\chi}_l^0}) + B_0(-p, m_t, m_{\tilde{\chi}_l^0}) m_t^2 + B_1(-p, m_t, m_{\tilde{\chi}_l^0}) p^2 \right) \right. \\
& + \left. 2 B_0(-p, m_t, m_{\tilde{\chi}_l^0}) m_t m_{\tilde{\chi}_l^0} \left(V_{t \tilde{t}_j \tilde{\chi}_l^0}^{(2)*} V_{t \tilde{t}_i \tilde{\chi}_l^0}^{(1)} + V_{t \tilde{t}_j \tilde{\chi}_l^0}^{(1)*} V_{t \tilde{t}_i \tilde{\chi}_l^0}^{(2)} \right) \right] \\
& - \sum_k^2 \left[2 \left(V_{b \tilde{t}_j \tilde{\chi}_k^+}^{(1)*} V_{b \tilde{t}_i \tilde{\chi}_k^+}^{(1)} + V_{b \tilde{t}_j \tilde{\chi}_k^+}^{(2)*} V_{b \tilde{t}_i \tilde{\chi}_k^+}^{(2)} \right) \left(A_0(m_{\tilde{\chi}_k^+}) + B_0(-p, m_b, m_{\tilde{\chi}_k^+}) m_b^2 + B_1(-p, m_b, m_{\tilde{\chi}_k^+}) p^2 \right) \right. \\
& + \left. 2 B_0(-p, m_b, m_{\tilde{\chi}_k^+}) m_b m_{\tilde{\chi}_k^+} \left(V_{b \tilde{t}_j \tilde{\chi}_k^+}^{(2)*} V_{b \tilde{t}_i \tilde{\chi}_k^+}^{(1)} + V_{b \tilde{t}_j \tilde{\chi}_k^+}^{(1)*} V_{b \tilde{t}_i \tilde{\chi}_k^+}^{(2)} \right) \right] \\
& - \sum_{\alpha, \beta}^2 \left[i A_0(m_{\tilde{t}_\alpha}) V_{\tilde{t}_i \tilde{t}_\alpha \tilde{t}_\alpha \tilde{t}_j} + i A_0(m_{\tilde{b}_\beta}) V_{\tilde{t}_i \tilde{b}_\beta \tilde{b}_\beta \tilde{t}_j} \right] \} \tag{A.5}
\end{aligned}$$

The top quark self-energy contributed by Fig.1(d1)-(d2) reads:

$$\Sigma_{tt}(p^2) = i(\not{p} \Sigma_{tt}^L P_L + \not{p} \Sigma_{tt}^R P_R + \Sigma_{tt}^{SL} P_L + \Sigma_{tt}^{SR} P_R), \tag{A.6}$$

where

$$\begin{aligned}
\Sigma_{tt}^L &= \frac{1}{16\pi^2} \left\{ - \sum_m^4 [(V_{H_m^0 tt})^2 B_1(-p, m_t, m_{H_m^0})] - \sum_n^2 [(V_{H_n^+ tb}^{(2)})^2 B_1(-p, m_b, m_{H_n^+})] \right. \\
&+ \left. \sum_k^2 \sum_\beta^2 [(V_{t \tilde{b}_\beta \tilde{\chi}_k^+}^{(2)})^2 (B_0 + B_1)(-p, m_{\tilde{b}_\beta}, m_{\tilde{\chi}_k^+})] + \sum_l^4 \sum_\alpha^2 [(V_{t \tilde{t}_\alpha \tilde{\chi}_l^0}^{(2)})^2 (B_0 + B_1)(-p, m_{\tilde{t}_\alpha}, m_{\tilde{\chi}_l^0})] \right\} \\
\Sigma_{tt}^R &= \Sigma_{tt}^L \left(V_{H_n^+ tb}^{(2)} \rightarrow V_{H_n^+ tb}^{(1)}, V_{t \tilde{b}_\beta \tilde{\chi}_k^+}^{(2)} \rightarrow V_{t \tilde{b}_\beta \tilde{\chi}_k^+}^{(1)}, V_{t \tilde{t}_\alpha \tilde{\chi}_l^0}^{(2)} \rightarrow V_{t \tilde{t}_\alpha \tilde{\chi}_l^0}^{(1)} \right) \\
\Sigma_{tt}^{SL} &= \frac{1}{16\pi^2} \left\{ - \sum_m^4 [(V_{H_m^0 tt})^2 m_t B_1(-p, m_t, m_{H_m^0})] + \sum_n^2 [V_{H_n^+ tb}^{(2)*} V_{H_n^+ tb}^{(1)} m_b B_1(-p, m_b, m_{H_n^+})] \right. \\
&+ \left. \sum_k^2 \sum_\beta^2 [V_{t \tilde{b}_\beta \tilde{\chi}_k^+}^{(2)*} V_{t \tilde{b}_\beta \tilde{\chi}_k^+}^{(1)} m_{\tilde{b}_\beta} B_0(-p, m_{\tilde{b}_\beta}, m_{\tilde{\chi}_k^+})] + \sum_l^4 \sum_\alpha^2 [V_{t \tilde{t}_\alpha \tilde{\chi}_l^0}^{(2)*} V_{t \tilde{t}_\alpha \tilde{\chi}_l^0}^{(1)} m_{\tilde{t}_\alpha} B_0(-p, m_{\tilde{t}_\alpha}, m_{\tilde{\chi}_l^0})] \right\} \\
\Sigma_{tt}^{SR} &= \Sigma_{tt}^{SL} \left(V_{H_n^+ tb}^{(2)*} V_{H_n^+ tb}^{(1)} \rightarrow V_{H_n^+ tb}^{(1)*} V_{H_n^+ tb}^{(2)}, V_{t \tilde{b}_\beta \tilde{\chi}_k^+}^{(2)*} V_{t \tilde{b}_\beta \tilde{\chi}_k^+}^{(1)} \rightarrow V_{t \tilde{b}_\beta \tilde{\chi}_k^+}^{(1)*} V_{t \tilde{b}_\beta \tilde{\chi}_k^+}^{(2)}, V_{t \tilde{t}_\alpha \tilde{\chi}_l^0}^{(2)*} V_{t \tilde{t}_\alpha \tilde{\chi}_l^0}^{(1)} \rightarrow V_{t \tilde{t}_\alpha \tilde{\chi}_l^0}^{(1)*} V_{t \tilde{t}_\alpha \tilde{\chi}_l^0}^{(2)} \right) \tag{A.7}
\end{aligned}$$

In our paper we adopt the definitions of the one-loop integrals in the references[24]. The numerical calculation of the vector and tensor one-loop integral functions can be traced back to four scalar loop integrals A_0, B_0, C_0, D_0 as shown in [25].

References

- [1] S.L. Glashow, Nucl. Phys. 22(1961)579; S. Weinberg, Phys. Rev. Lett. 1(1967)1264; A. Salam, Proc. 8th Nobel Symposium Stockholm 1968, ed. N. Svartholm(Almquist and Wiksells, Stockholm 1968) p.367; H.D. Politzer, Phys. Rep. 14(1974)129.
- [2] P.W. Higgs, Phys. Lett 12(1964)132, Phys. Rev. Lett. 13 (1964)508; Phys.Rev. 145(1966)1156; F.Englert and R.Brout, Phys. Rev. Lett. 13(1964)321; G.S. Guralnik, C.R.Hagen and T.W.B. Kibble, Phys. Rev. Lett. 13(1964)585; T.W.B. Kibble, Phys. Rev. 155(1967)1554.
- [3] H. E. Haber, G. L. Kane, Phys. Rep. 117(1985) 75.
- [4] J.Ellis and S.Rudaz, Phys. Lett. B128(1983)248; J.F.Gunion and H.E.Haber, Nucl. Phys. B272(1986)1.
- [5] J. Ellis and S.Rudaz, Phys. Lett. B128(1983)248.
- [6] H. Baer, B. Barger, D. Laratas and X. Tata. Phys. Rev.D36, (1987) 96; K. Hikasa and M. Kobayashi, Phys. Rev. D36, (1987) 724; R.M. Barnett, J.F. Gunion and H.E. Harber, Phys. Rev. D37, (1988) 1892; H. Baer, X. Tata and J. Woodside, Phys. Rev. D42, (1990) 1568; K. Hikasa and M. Drees, Phys. Lett. B252 (1990) 127; A. Bartl, W. Majerotto, B. Mösslacher and N. Oshimo, Z. Phys. C52, (1991) 477; A, Bartl, W. Majerotto and W. Porod, Z. Phys. C64,(1994) 499.
- [7] A. Bartl, H. Eberl, K. Hidaka, S. Kraml, T. Kon, W. Majerotto, W. Porod and Y.Yamada, Phys. Lett. B435 (1998) 118.
- [8] A. Djouadi, W. Hollik and C. Junger, Phys.Rev. D55 (1997) 6975.
- [9] A. Djouadi, W. Hollik and C. Junger, Phys.Rev. D54 (1996) 5629.
- [10] J. Guasch, W. Hollik and J.Solà, Phys. Lett. B437, (1998) 88.

- [11] J. Guasch, W. Hollik and J.Solà, Phys. Lett. B510 (2001) 211.
- [12] A. Bartl, H. Eberl, K. Hidaka, S. Kraml, W. Majerotto, W. Porod and Y.Yamada, hep-ph/9806229.
- [13] L.G. Jin and C.S. Li, hep-ph/0106253.
- [14] W. Beenakker, R. Höpker and P.M. Zerwas, Phys.Lett. B378 (1996) 159.
- [15] W. Beenakker, R. Höpker R. Plehn and P.M. Zerwas, Z.Phys. C75 (1997) 349.
- [16] W. Beenakker, R. Höpker, M. Spira and P.M. Zerwas,Z.Phys. C69 (1995) 163.
- [17] W. Beenakker and R. Höpker, Nucl. Phys. Proc. Suppl. 51C (1996) 261.
- [18] G.L. Kane and S. Mrenna, Phys.Rev.Lett. 77 (1996) 3502.
- [19] D.M. Copper, D.R.T. Jones and P. van Nieuwenhuizen Nucl. Phys. **B167** 479(1980); W. Siegel, Phys. Lett. **B84** 193(1979).
- [20] A. Denner, Fortschr. Phys. **41** (1993) 307.
- [21] M. Böhm, H. Spiesberger, W. Hollik, Fortsch. Phys. **34** (1986) 687; W. Hollik, Fortschr. Phys. **38**(1990) 165.
- [22] Particle Data Group, Eur. Phys. J. **C15** 2000.
- [23] M.L. Zhou, W.G. Ma, L. Han, Y. Jiang and H. Zhou, J. Phys. **G25** 1641(1999)
- [24] Bernd A. Kniehl, Phys. Rep. **240** 211(1994).
- [25] G. Passarino and M. Veltman, Nucl. Phys. **B160**, 151(1979)

Figure Captions

Fig.1 Feynman diagrams including one-loop Yukawa corrections to the decays $\tilde{t}_j \rightarrow \tilde{g} + t$ and $\tilde{g} \rightarrow \bar{t} + \tilde{t}_j$: Fig.1(a) tree-level diagram. Fig.1(b) vertex corrections for stop decays. Fig.1(c) stop quark self-energies. Fig.1(d) top quark self-energies. In these Figures $H_m^0 = h^0, H^0, A^0, G^0 (m = 1 - 4)$ and $H_n^+ = H^+, G^+ (n = 1, 2)$.

Fig.2 The relative correction for $\tilde{t}_2 \rightarrow \tilde{g} + t$ as a function of $m_{\tilde{g}}$.

Fig.3 The relative correction for $\tilde{t}_2 \rightarrow \tilde{g} + t$ as a function of $m_{1/2}$ in the mSUGRA scenario.

Fig.4 The relative correction for $\tilde{g} \rightarrow \bar{t} + \tilde{t}_1$ as a function of $m_{\tilde{g}}$.

Fig.5 The relative correction for $\tilde{g} \rightarrow \bar{t} + \tilde{t}_1$ as a function of $m_{1/2}$ in the mSUGRA scenario.

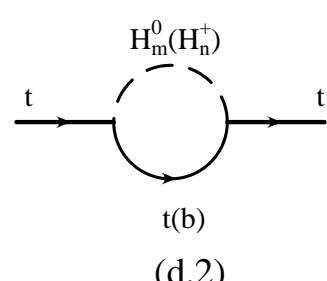
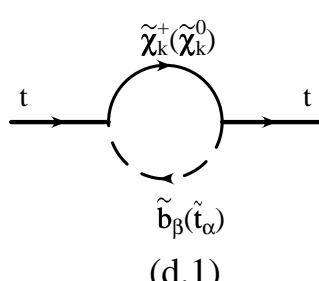
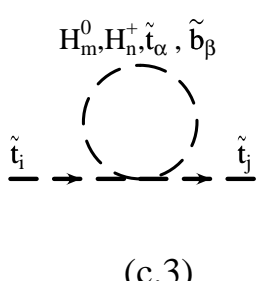
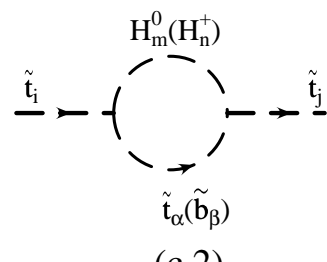
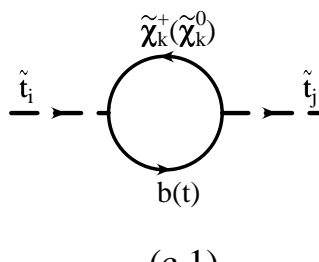
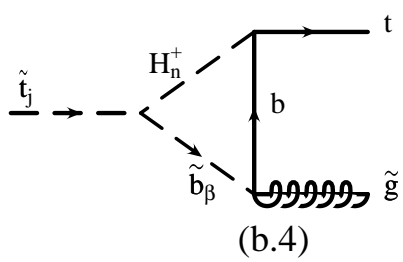
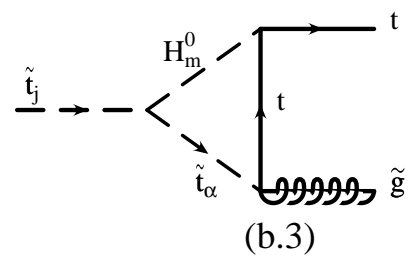
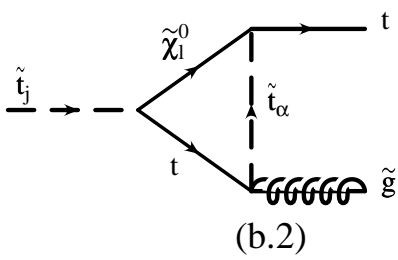
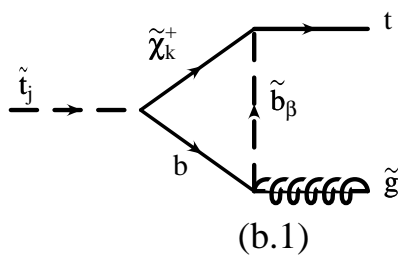
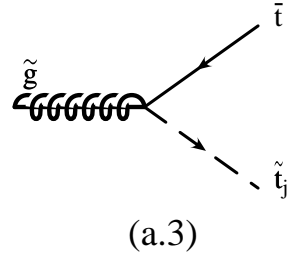
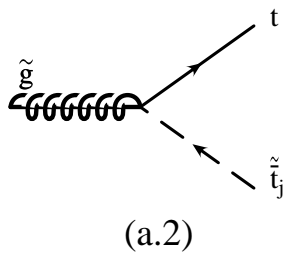
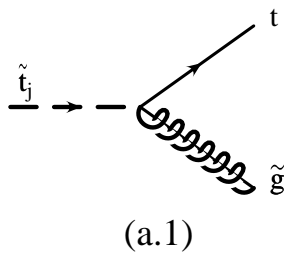


Figure. 1

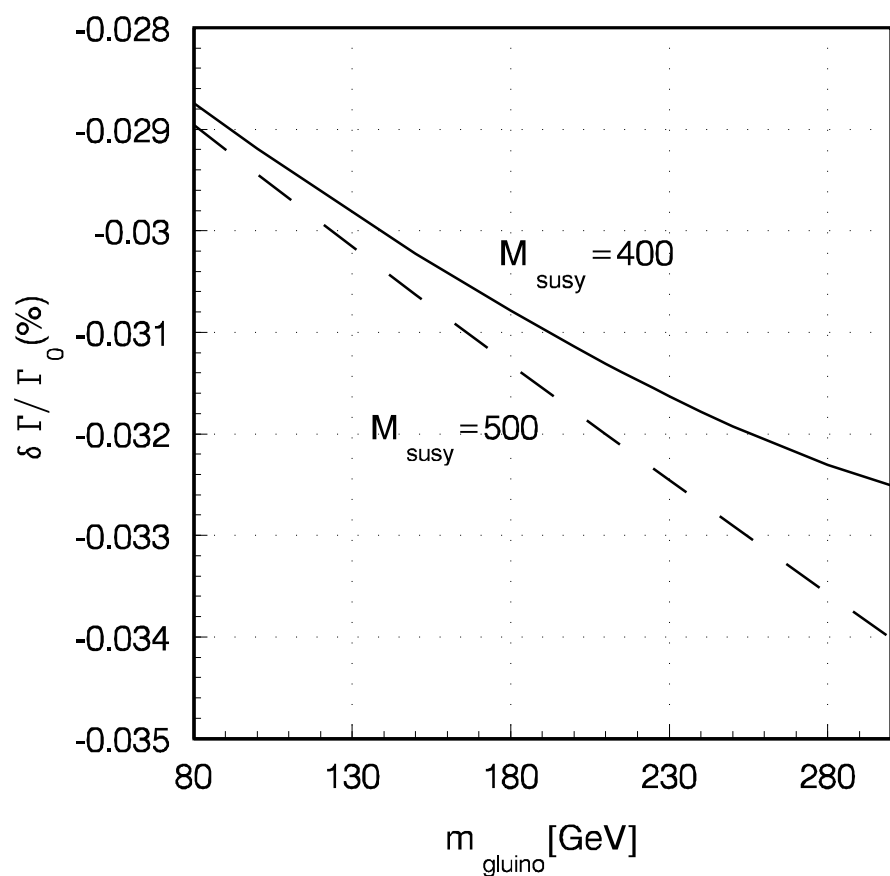


Fig.2

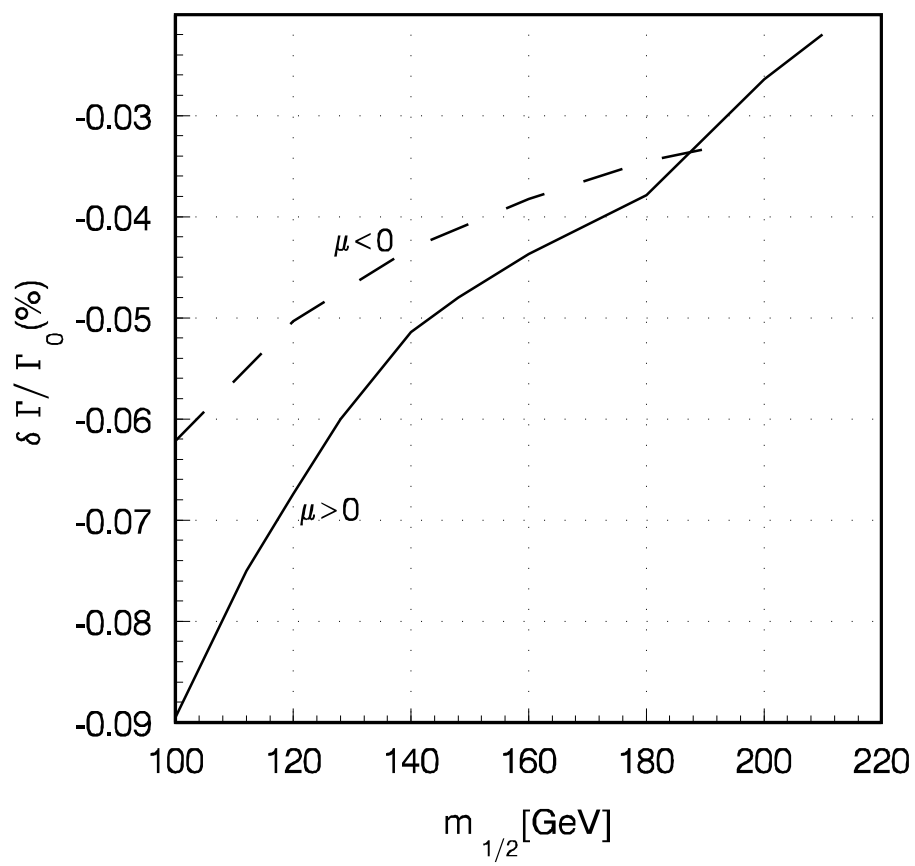


Fig.3

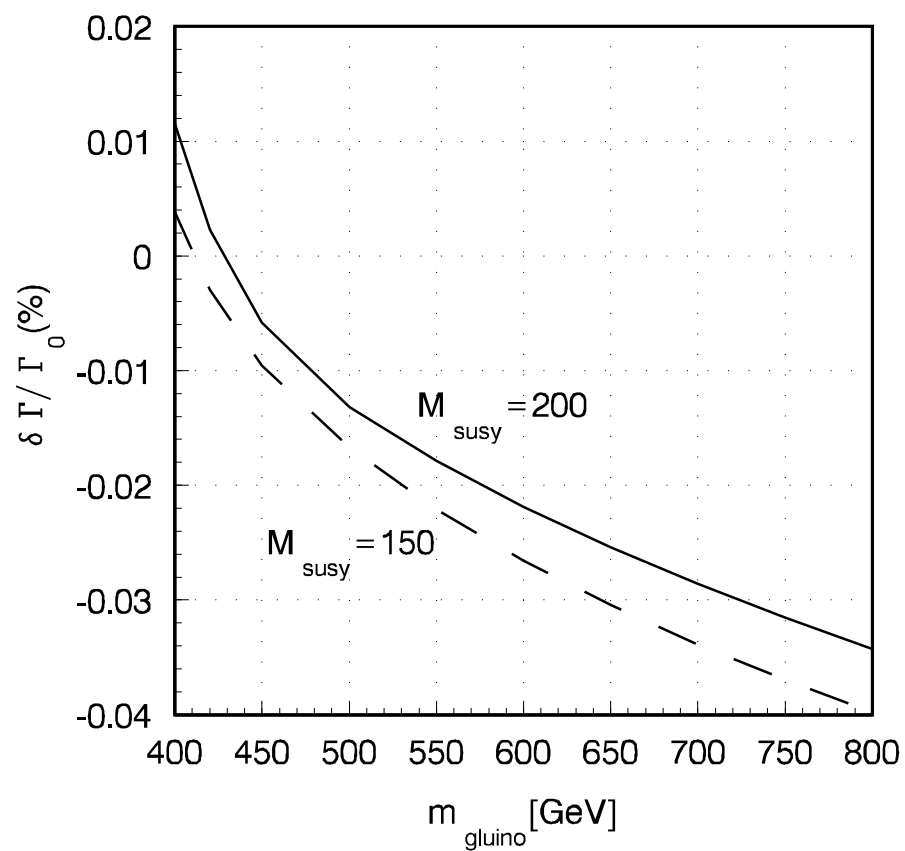


Fig.4

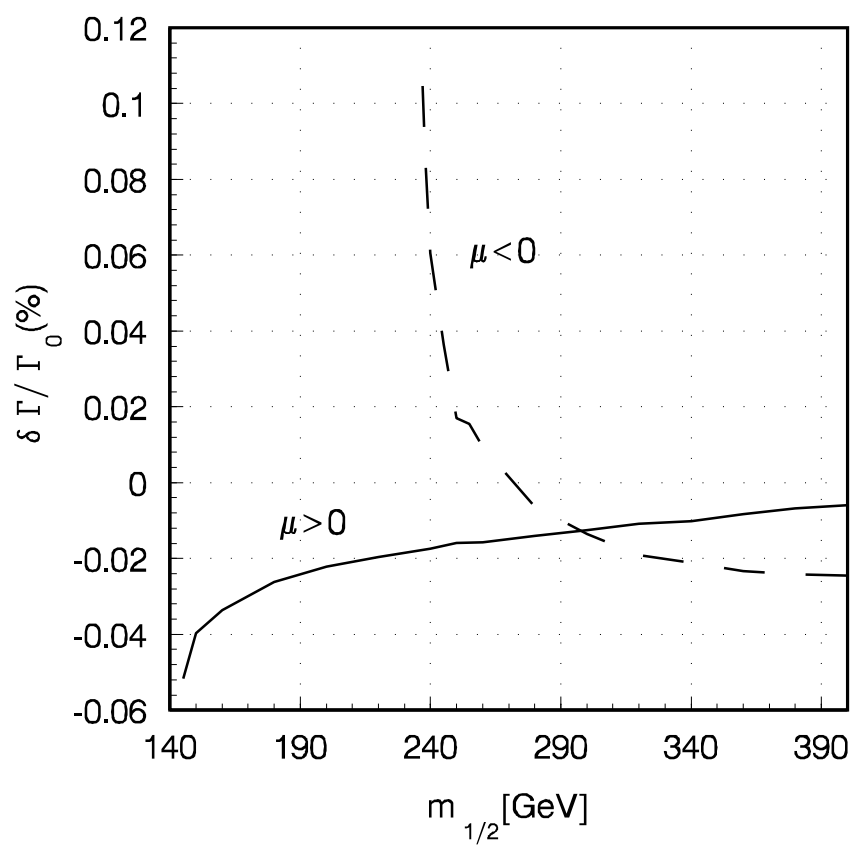


Fig.5